processes

MDPI

*Article*

# Thermo-Mechanical Behavior of Green Sandwich Structures for Building and Construction Applications

**Forhad Hossain [1], Md Arifuzzaman [1,*], Md Shariful Islam [1] and Md Mainul Islam [2]**

[1] Department of Mechanical Engineering, Khulna University of Engineering & Technology, Khulna 9203, Bangladesh; forhadakib101@gmail.com (F.H.); msislam@me.kuet.ac.bd (M.S.I.)
[2] School of Engineering and Centre for Future Materials, University of Southern Queensland, Toowoomba, QLD 4350, Australia; mainul.islam@usq.edu.au
* Correspondence: arif48@me.kuet.ac.bd

**Abstract:** In this work, three different types of sandwich structures were manufactured, each using a Formica sheet (a paper-based sheet) as the skin and perlite/sodium silicate foam as the core, with or without a paper honeycomb. The sandwich structures were fabricated by attaching the Formica sheets on both sides of a paper honeycomb core panel, a perlite/sodium silicate foam core panel, and a perlite/sodium silicate foam-filled honeycomb core panel. The flexural characteristics were studied by a three-point bending test and the thermal conductivity was measured using Lee's thermal conductivity apparatus. The results demonstrated a significant improvement in flexural properties, including core shear stress, facing stress, bending stress, and energy absorption, when incorporating the paper honeycomb reinforcement. The thermal conductivity and flexural properties of the paper honeycomb reinforced and unreinforced perlite/sodium silicate foam-based sandwich panels were found to be very compatible with existing building materials described in the literature that are used for similar applications. The failure investigation revealed that the sandwiches with paper honeycomb failed prematurely only due to core buckling, while the foam-filled honeycomb core-based sandwiches were able to sustain higher loads while exhibiting material failures such as core shear failure, skin rapture, and delamination. It was found that the foam-filled paper honeycomb sandwich structures can withstand higher bending loads than the foam core-based sandwich structure or the paper-honeycomb-based sandwich structure. These developed sandwiches offer potential as green materials due to the characteristics of their constituent materials and they can provide valuable applications in the thermal insulation of buildings.

**Keywords:** perlite composite-filled paper honeycomb sandwich; thermal insulation board; green sandwich structure; flexural properties; thermal conductivity



**Citation:** Hossain, F.; Arifuzzaman, M.; Islam, M.S.; Islam, M.M. Thermo-Mechanical Behavior of Green Sandwich Structures for Building and Construction Applications. *Processes* **2023**, *11*, 2456. https://doi.org/10.3390/pr11082456

Academic Editor: Jacopo Donnini

Received: 26 July 2023
Revised: 12 August 2023
Accepted: 13 August 2023
Published: 15 August 2023



## 1. Introduction

Expanded perlite is a lightweight material that is used extensively because of its appealing chemical and physical characteristics. The raw perlite particles obtained from the obsidian typically increase in volume by 5–20 times when rapidly heated to a temperature of 900 °C to 1200 °C [1]. They are used in construction industries because of their low bulk density [2] and their attractive properties. Expanded perlite particles are environmentally friendly and chemically inert. They possess strong heat and fire resistance, low thermal conductivity, and good sound insulation characteristics [3–5].

The uses of expanded perlite particles for the development of building materials were covered extensively in a review by Rashad [6]. Expanded perlite particle-based building boards were studied by many researchers, including fiber/asphalt coated perlite building boards studied by Miscall and Rahr [7]; mineral board studied by Sherman and Cameron [8]; perlite/starch foam studied by Shastri and Kim [9]; gypsum/perlite composite studied by Vimmrova [10] and Karua and Arifuzzaman [11]; perlite/sodium

silicate board studied by Arifuzzaman and Kim [12–15], Adhikary et al. [16], Karua and Arifuzzaman [17], Takey et al. [18], Tian et al. [19], and Abir et al. [20]; and perlite and vermiculate based lightweight fire-rated board studied by Yew et al. [21].

Perlite/sodium silicate foam boards may be an alternative to gypsum board because of their light weight, high strength-to-weight ratio, and better thermal and acoustic insulation. The concentration of sodium silicate in perlite-based foams plays a vital role in the physical and mechanical properties of perlite/sodium silicate foam boards. It was found from the literature that the density and the compressive and flexural strength of expanded perlite boards increase linearly with increasing concentrations of sodium silicate [12,14,19]. The effect of sodium silicate binder and the compaction ratio on the mechanical properties of perlite-based building boards was broadly studied by Arifuzzaman and Kim [12,13]. One of the important characteristics of perlite/sodium silicate composite foam is that the failure of perlite/sodium silicate panels initiates on a specimen's tensile side [13] during flexural loading, causing a lower load-bearing capacity and decreased toughness of the panels. However, Arifuzzaman and Kim [22] found that the failure side was shifted to the mid-plane of the flexural specimen when brown paper was used as a skin reinforcement for the sandwich structure. The load-bearing capacity of the structure also increased, by roughly 3–7 times. Therefore, sandwiching perlite/sodium silicate composite foams with various skins could influence the flexural properties of a structure, based on the skins' material properties.

Paper honeycomb sandwich panels have been used to package large-scale goods, furniture, building materials, and other things due to their light weight, high strength, and cushioning characteristics [23–25]. The paper honeycomb sandwich structures for building applications were studied in the past [26–29]. For example, Shahbazi et al. [26] investigated a sandwich structure made of flax fiber-reinforced Portland cement and kraft paper honeycomb as the face sheet and the core material, respectively. The flexural and thermal properties were found to be compatible with those of traditional gypsum boards. Kadir et al. [28] examined an effective method for finding the ideal arrangement of kraft paper honeycomb. They studied the effects of paper density, cell-wall thickness, and honeycomb cell size on specific energy absorption and specific compressive strength. Their findings showed that all parameters had a discernible impact, but the width of the cell wall had the greatest impact on the functionality of kraft paper honeycomb.

The effects of foam filling on the behavior and failure of sandwich panels made of a paper honeycomb core are limited. Fu and Sadeghian [27] found that filling paper honeycomb core cells with polyurethane foam increased the load-bearing capacity of the sandwiches [27]. Kadir et al. [28] also used low-density polyurethane to fill kraft paper honeycomb cells. They showed that adding polyurethane foam to the kraft paper honeycomb helped to reinforce the cell walls, which in turn increased both the honeycomb's capacity to absorb energy and the peak force. Therefore, filling paper honeycomb core cells with lightweight expanded perlite foams could benefit the load-bearing capacity and toughness of the sandwiches.

The face sheet material has a significant impact on the flexural properties of a sandwich structure. For example, Safarabadi et al. [30] studied the buckling behavior of a Nomex honeycomb core with glass-epoxy face sheet sandwich panels for both bare and foam-filled cores. They reported that the presence of foam increased the crucial buckling load. The characteristics of the face sheets had a greater influence on the buckling behavior and the energy absorption or toughness of the composite panel.

Studies of sandwich structures made of the expanded perlite-based core are limited in the literature. Arifuzzaman and Kim [22] studied the flexural behavior of expanded perlite/sodium silicate core-based sandwich structures using brown paper as the skin. Recently, Sarkar et al. [31] and Hossain et al. [32] investigated sandwich structures using jute fiber-reinforced epoxy composite as the skin and expanded perlite/epoxy and expanded perlite/sodium silicate as the cores, respectively. Formica sheets made of high-grade craft paper may be a good candidate for the skin of the perlite/sodium silicate core-based

sandwich structure. Notably, Formica sheets are widely used in the furniture industries and in building interior decoration.

In this work, novel green sandwich structures were formulated using expanded perlite/sodium silicate foam, paper honeycomb, and perlite/sodium silicate foam-filled paper honeycomb cores, with Formica sheet as the skin. The flexural and thermal behavior of the manufactured composites were investigated and compared with similar existing building materials that are discussed in the literature.

## 2. Materials and Method

### *2.1. Materials*

For manufacturing perlite foam-filled honeycomb sandwich structures, the honeycomb structure was made using kraft paper, and the cells of the paper honeycomb structures were filled with perlite/sodium silicate composite foam. Formica sheets were used as the skins of the sandwich structures. The skins were bonded to the cores using a synthetic resin adhesive (Fevicol SH). A schematic of the sandwich structure considered in this study is shown in Figure 1.

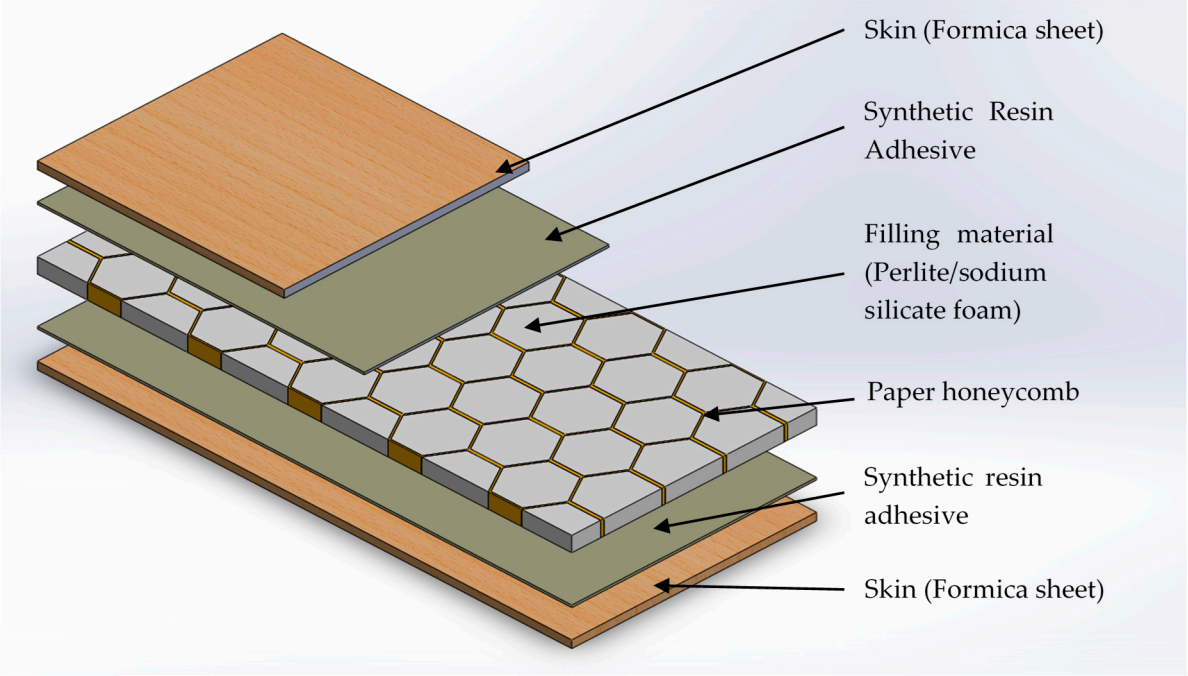


**Figure 1.** A schematic view of the honeycomb sandwich structure considered in this study.

Kraft liner paper with an average thickness of 0.49 mm was purchased from the local market. Glossy-finished Formica sheets, "Formica & Ebonite (HPL) 717" of thickness 0.50 mm (Super Formica & Lamination Limited, Jamaldi, Bangladesh), were purchased from a local supplier. According to the manufacturer, the raw materials of Formica sheets are high-grade kraft paper, phenol formaldehyde, and melamine formaldehyde resin. The sheets are scratch-resistant and have firm, slick surfaces. Multiple layers of impregnated paper are fused under high temperature and high pressure to manufacture Formica sheets. They are tough, long-lasting, and non-toxic to humans. The tension test for the Formica sheets was conducted with a Universal testing machine (Shimadzu AGX 300 kNV, Kyoto, Japan) at a crosshead speed of 5 mm/min to determine the tensile properties. The coupon specimen's dimensions were 250 mm × 25 mm. The stress-strain curves for five specimens are shown in Figure 2. All specimens showed a similar trend consisting of a linear increase in stress with strain up, to a peak where a brittle tearing took place. The average values of tensile strength, modulus, and failure strain with standard deviations are provided in Table 1.

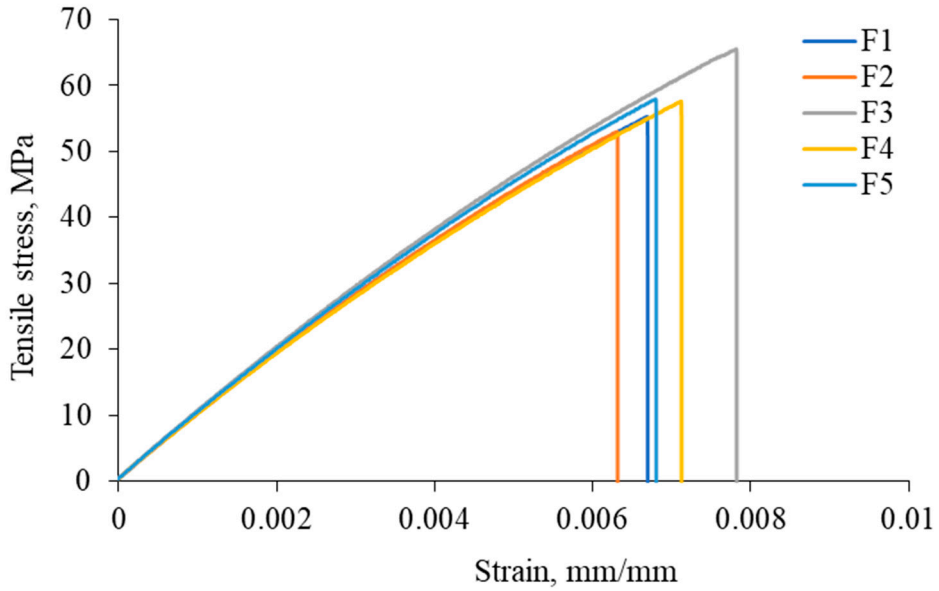


**Figure 2.** Tensile stress-strain curves of Formica sheet.

**Table 1.** Tensile properties of Formica sheet.

| Sample | Tensile Strength (MPa) | Tensile Modulus (GPa) | Failure Strain (%) |
|---|---|---|---|
| Formica sheet | 57.89 ± 4.73 | 8.91 ± 0.23 | 0.69 ± 0.05 |

Expanded perlite particles were purchased from Xinyang Caster New Material Co., Ltd. (Xinyang, China). The particles were sorted into sizes ranging from 2.36 mm to 4.75 mm, using sieves to maintain uniformity. The powders and particles of sizes other than 2.36 to 4.75 mm were filtered out. According to the manufacturer's catalog, the expanded perlite contained 70–75% $SiO_2$, 12–16% $Al_2O_3$, 2.5–5% $Na_2O$, 1–4% $K_2O$, 0.1–2% CaO, 0.15–1.5% $Fe_2O_3$, and 0.2–0.5% MaO.

Sodium silicate solution (SSS) was supplied by Silica Solution, a concern of Rupam Soap & Chemical Industries Ltd., (Chattogram, Bangladesh). The manufacturer's datasheet stated that the weight ratio of sodium oxide and silicon dioxide was 1:3.2, and that the solution had a density of 1.381 g/cm$^3$ at 20 °C. The solution contained 36.3 ± 1.2% of solid sodium silicate (by weight). To vary the solid content further, the SSS was diluted with 10% and 20% drinking water. The sample identifications (IDs) and the SSS dilutions are shown in Table 2. In the sample IDs in Table 2, "FHCS" and "FCS" refer, respectively, to a perlite/sodium silicate foam-filled paper honeycomb sandwich structure and a perlite/sodium silicate foam core sandwich structure.

**Table 2.** Dilution of sodium silicate solution for different samples.

| Sample ID | Sodium Silicate Solution, wt.% | Water, wt.% |
|---|---|---|
| FHCS-100, FCS-100 | 100 | 0 |
| FHCS-90, FCS-90 | 90 | 10 |
| FHCS-80, FCS-80 | 80 | 20 |

### *2.2. Specimen Preparation*

#### 2.2.1. Fabrication of Honeycomb Structure

The process of fabricating the sandwich structure consists of several steps, including paper-honeycomb-structure fabrication, perlite-foam manufacturing, filling honeycomb cells, curing, and attaching skins. The hexagonal shape was chosen for the paper honeycomb to obtain better performance [33]. The paper honeycombs were fabricated by the

traditional expansion process [34]. The fabrication process of a paper honeycomb structure is shown in Figure 3. Kraft paper was cut into strips of 12 mm wide and 320 mm long, using a paper cutter. The paper strips were marked as shown in Figure 3c, with intervals of 20 mm. Glue (Fevicol SH) was applied to the strips at intervals of 60 mm and 20 strips were stacked together in such a way that the glued portion of one strip did not coincide with an adjacent strip. After curing for 24 h, the final step was to pull the strips apart to expand the stacked strips into a hexagonal honeycomb structure, as shown in Figure 3e. The dimensions of the honeycomb cells are shown in Figure 3f.

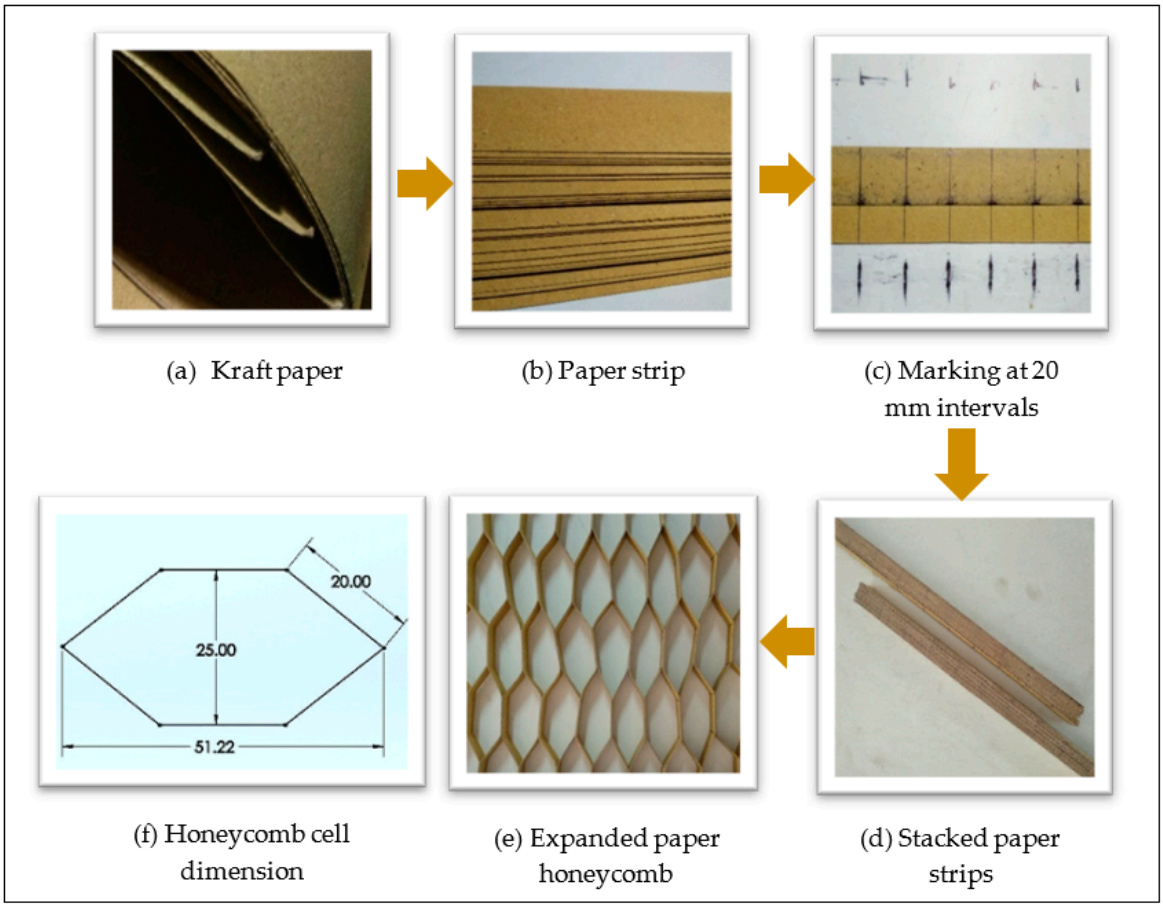


**Figure 3.** Fabrication process for the paper honeycomb structure.

### 2.2.2. Preparation of Perlite Foam Mixture

Figure 4 schematically shows the process of making the perlite/sodium silicate foam mixture. The SSS was diluted using drinking water, as presented in Table 2. Dry perlite particles were placed in a container and the diluted SSS was poured into the container, followed by hand mixing for 5 min, which was sufficient to obtain a uniform mixture. The mixing proportion of the perlite, water, and sodium silicate solution for different samples is provided in Table 3. A slightly higher amount of perlite particles (5 g, as shown in Table 3) was used to manufacture sandwich cores without paper honeycomb to compensate for the density change. However, the total ratio of SSS to perlite particle was kept constant at 4.29. The prepared foam mixture was later used to manufacture perlite/sodium silicate foam-filled paper honeycomb and perlite/sodium silicate foam panels, as described in the following section.

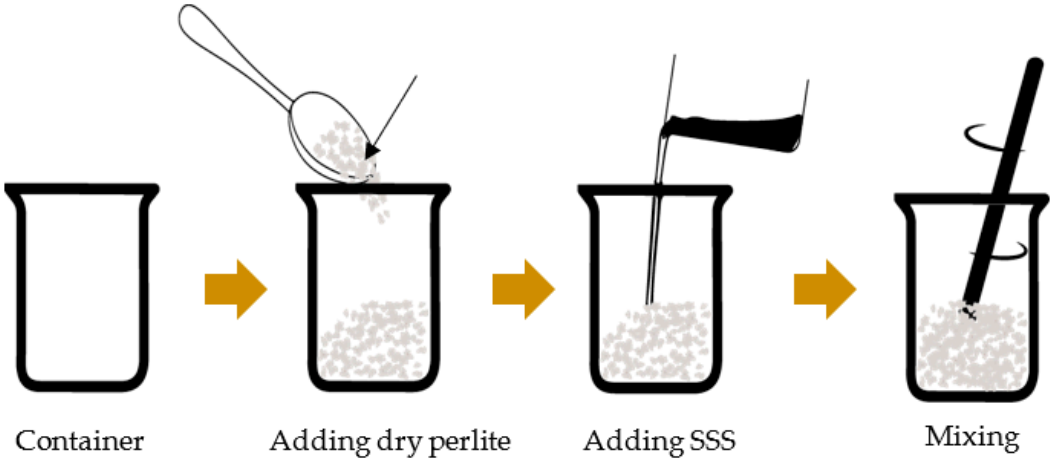


**Figure 4.** Steps for preparing perlite/sodium silicate foam mixture.

**Table 3.** Amount of the constituents used to prepare perlite/sodium silicate foam mixture.

| Sample ID | Mass of Perlite (g) | Mass of SSS as Received (g) | Mass of Water (g) | Mass of Diluted SSS (g) |
|---|---|---|---|---|
| FHCS-100 | 85 | 365.00 | 0 | 365.00 |
| FCS-100 | 90 | 386.47 | 0 | 386.47 |
| FHCS-90 | 85 | 328.50 | 36.50 | 365.00 |
| FCS-90 | 90 | 347.82 | 38.65 | 386.47 |
| FHCS-80 | 85 | 292.00 | 73.00 | 365.00 |
| FCS-80 | 90 | 309.18 | 77.29 | 386.47 |

#### 2.2.3. Core Manufacturing

The expanded honeycomb structure was placed into a mold with dimensions of 250 mm × 250 mm; then, the perlite/sodium silicate foam mixture was manually poured into the cells of the honeycomb structure. The top surface of the filled mold was made plain, using a metal bar and applying light compaction. The wet foam-filled mold was then placed inside an electric oven at 80 °C for 24 h to cure. A load of approximately 4 kg was kept on the top of the wet foam-filled honeycomb to resist the bending of the core during curing. After curing, the bottom surface of the core was found to be smooth and the paper honeycomb edges were visible. However, the top surface was rough and the paper honeycomb edges were not visible, because some of the particles were broken and remained on top of the paper honeycomb when the compaction was applied using the metal bar. To ensure proper adhesion of the paper honeycomb edges to the sandwich skin, it was necessary to polish the top surface, using emery paper, to make the paper honeycomb edges visible. A photograph of the manufactured foam-filled paper honeycomb core is provided in Figure 5a. For manufacturing perlite/sodium silicate foam panels without paper honeycomb, the wet mixture of the perlite and sodium silicate was poured into the mold and the top surface was leveled, using the metal bar. After that, the curing process was the same as that used for the foam-filled paper honeycomb cores. The manufactured perlite/sodium silicate foam-filled honeycomb panels and the perlite/sodium-silicate-foam-only panels were used to fabricate the sandwich structures, as described in the following section.

#### 2.2.4. Fabrication of Sandwich

The Formica sheets were cut into rectangular shapes of 250 mm × 250 mm, which was the internal size of the mold. The Formica sheets were attached to both surfaces of the core, with 20 g of adhesives on the rough surface of each sheet. The adhesive was evenly distributed, using a brush. The Formica skins were attached by keeping the longitudinal direction of the honeycomb cells aligned with the longitudinal direction of the Formica sheets. To minimize distortion, the sandwich specimens were further sandwiched between

two flat glass plates of 6 mm thickness, and a load of approximately 4 kg was placed above the top glass plate. The sandwich was left for 24 h so that the adhesive could cure. A representative photograph of a foam core sandwich without a paper honeycomb is shown in Figure 5b. The sandwich structures were cut into 250 mm × 80 mm shapes along the longitudinal direction, using a circular saw for testing.


(**a**) (**b**)

**Figure 5.** Photograph of (**a**) perlite/sodium silicate foam-filled paper honeycomb core and (**b**) sandwich structure made of perlite/sodium silicate foam core with Formica sheet as skin.

### *2.3. Density Measurement*

The lengths, widths, and thicknesses of the samples were measured using digital slide calipers (Mitutoyo 0–300 mm, Kawasaki, Japan) with an accuracy of 0.01 mm. The mass of the samples was measured using a 0.01–300 g weighing machine (AND Company Ltd., Seoul, Republic of Korea) with an accuracy of 0.01 g. The density of the samples was determined using the following equation:

$$\rho = \frac{M}{V}, \tag{1}$$

where ρ, M, and V are the density, mass, and volume of the specimens, respectively.

### *2.4. Flexural Testing*

Three-point bending tests were conducted with a universal testing machine (Shimadzu AGX-300kNV, Japan) at a crosshead speed of 6 mm/min and a support-span length of 150 mm, according to standard ASTM C393/C393M-11 [35]. Figure 6 shows a schematic diagram of the three-point bending test arrangement. The diameters of the loading roller and the support rollers were 10 mm and 30 mm, respectively. At least three specimens were tested for sandwiches with only a foam core; six specimens were tested for sandwiches with a foam-filled paper honeycomb core. The data (load and deflection) were recorded using the data acquisition software TrapeziumX-V, Version 1.0.6 by Shimadzu, Japan, at an interval of 0.05 s. The ultimate core shear strength ($F_s$) and the average facing strength ($\sigma_{skin}$) were calculated using Equations (2) and (3), respectively, according to ASTM C393/C393M-11.

$$F_s = \frac{P}{(d + c)b} \tag{2}$$

$$\sigma_{skin} = \frac{PS}{2t(d + c)b} \tag{3}$$

where P, S, b, d, t, and c are the applied load, support span length, specimen width, specimen depth, skin thickness, and core thickness, respectively.

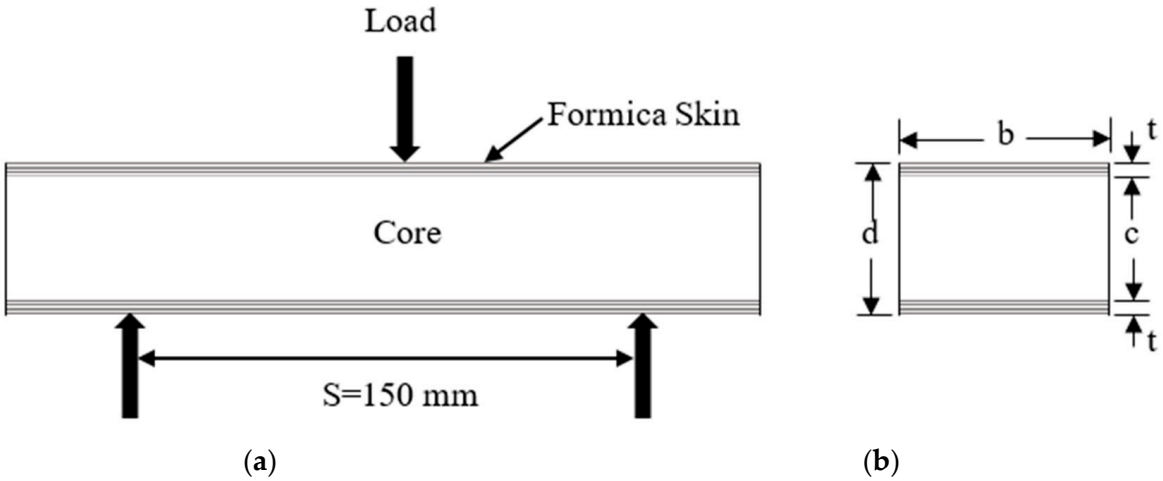


**Figure 6.** A schematic diagram of (**a**) flexural test setup and (**b**) dimension convention of the sandwich cross-section.

### *2.5. Thermal Conductivity Testing*

Lee's disc method [36] is well-known for measuring the thermal conductivity of the insulation material that was used to determine the thermal conductivity of the sandwiches. For the thermal conductivity test, the samples were cut into circular shapes with diameters of 100 mm. Figure 7 shows the experimental setup for the thermal conductivity test. The following equation was used to determine thermal conductivity:

$$k = \frac{mS\left(\frac{dT}{dt}\right)x}{A(T_2 - T_1)} \quad (4)$$

where m, S, x, and A are the mass of the lower disc, the specific heat capacity of brass, the slope of the cooling curve, the specimen thickness, and the area of the specimen, respectively. The detailed procedure for measuring thermal conductivity, using Lee's disc method, can be found in [36].

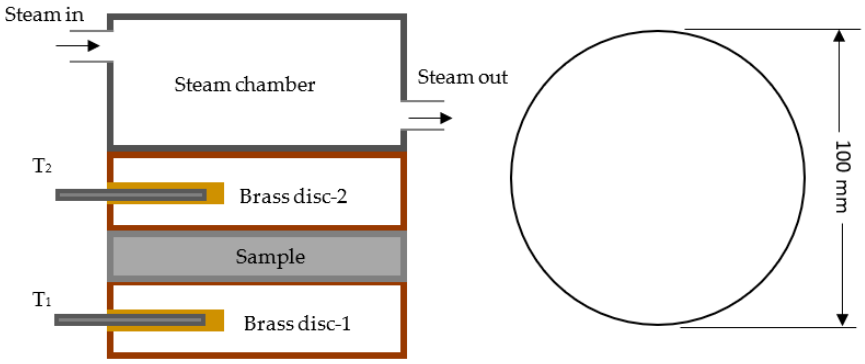


**Figure 7.** A schematic diagram of the thermal conductivity test setup.

## 3. Results and Discussion

### *3.1. Flexural Properties*

The density, core shear stress, facing stress, flexural modulus, equivalent flexural strength, and thermal conductivity of different samples are provided in Table 4. The sample ID "HCS" in Table 4 indicates the sandwich structure with only a paper honeycomb core. The densities of the prepared sandwiches are shown as a bar chart in Figure 8, with standard deviation indicated by the error bars. The range of density of the sandwiches with and without paper honeycomb was found to be from 0.40 g/cm$^3$ to 0.47 g/cm$^3$. The density of

the sandwiches appeared to be slightly decreasing with the decreasing solid content in the SSS via dilution. Comparing the density of the FHCSs and the FCSs, the density of the FCSs was slightly lower than that of the FHCSs, although extra perlite was used in the FCSs. The insignificant deviation in density was favorable for comparing the mechanical properties of the sandwiches. For the sandwich with only a paper honeycomb core, the density was found to be 0.15 g/cm$^3$, which was 62.5% lower than the lowest-density sandwich (e.g., FCS-80) in this study.

**Table 4.** Flexural characteristics of sandwich structures.

| Sample ID | Density, g/cm$^3$ | Core Shear Stress, MPa | Facing Stress, MPa | Flexural Modulus, GPa | Flexural Strength, MPa | Thermal Conductivity, W/mK |
|---|---|---|---|---|---|---|
| FHCS-100 | 0.47 ± 0.010 | 0.35 ± 0.10 | 51.26 ± 13.81 | 1.76 ± 0.09 | 11.03 ± 2.95 | 0.10 ± 0.010 |
| FHCS-90 | 0.44 ± 0.003 | 0.27 ± 0.02 | 39.72 ± 3.00 | 1.61 ± 0.07 | 8.55 ± 0.64 | 0.11 ± 0.003 |
| FHCS-80 | 0.42 ± 0.007 | 0.20 ± 0.06 | 28.64 ± 7.65 | 1.30 ± 0.09 | 6.26 ± 1.70 | 0.10 ± 0.010 |
| FCS-100 | 0.46 ± 0.009 | 0.23 ± 0.05 | 33.69 ± 6.86 | 1.44 ± 0.09 | 7.79 ± 1.62 | 0.11 ± 0.010 |
| FCS-90 | 0.43 ± 0.006 | 0.22 ± 0.03 | 31.53 ± 4.36 | 1.19 ± 0.14 | 7.45 ± 1.08 | 0.11 ± 0.010 |
| FCS-80 | 0.40 ± 0.011 | 0.13 ± 0.03 | 18.95 ± 3.85 | 1.07 ± 0.21 | 4.06 ± 0.82 | 0.09 ± 0.004 |
| HCS | 0.15 ± 0.008 | 0.04 ± 0.02 | 4.59 ± 1.81 | 0.22 ± 0.12 | 1.01 ± 0.40 | - |

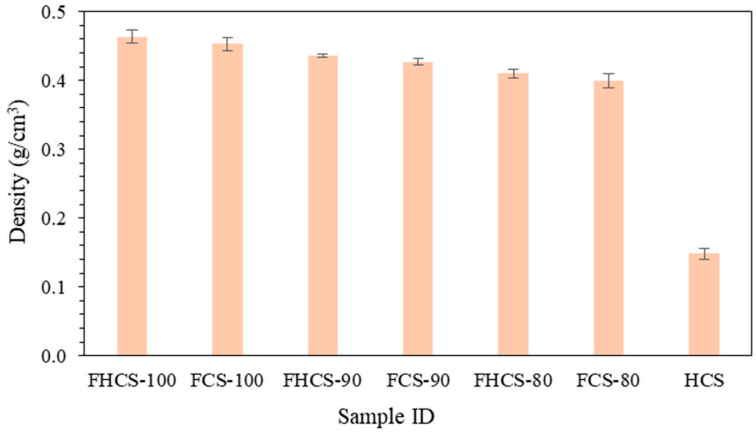


**Figure 8.** Density of various sandwich structures.

The flexural strength and the modulus of the sandwich structures are shown in Figure 9. As expected, the flexural strength and modulus decreased with the decrease in the concentration of the solid content in the SSS, due to the dilution for both types of sandwiches (i.e., sandwiches with and without paper honeycomb). The flexural strength and modulus of the FHCSs were found to be higher than those of the FCSs for each SSS concentration. The flexural strength of the FHCSs increased by 41.65%, 14.68%, and 54.12% for SSS concentrations of 100%, 90%, and 80%, respectively, compared to the respective FCSs. The improvement in the flexural modulus of FHCSs was 22.05%, 35.01%, and 21.00% for SSS concentrations of 100%, 90%, and 80%, respectively. The flexural strength of the HCS was found to be 1.01 MPa, which was significantly lower than that of other sandwiches in this study. The flexural strength and modulus of the HCS increased considerably, due to foam filling. The flexural strength of the FHCSs made by filling perlite/sodium silicate composite foams of 100%, 90%, and 80% SSS concentrations increased by 998.85%, 751.75%, and 523.74%, respectively, compared to that of the HCS. The flexural modulus of the HCS increased by 734.66%, 665.35%, and 516.24%, respectively, due to filling with perlite/sodium silicate foams manufactured with 100%, 90%, and 80% SSS concentrations.

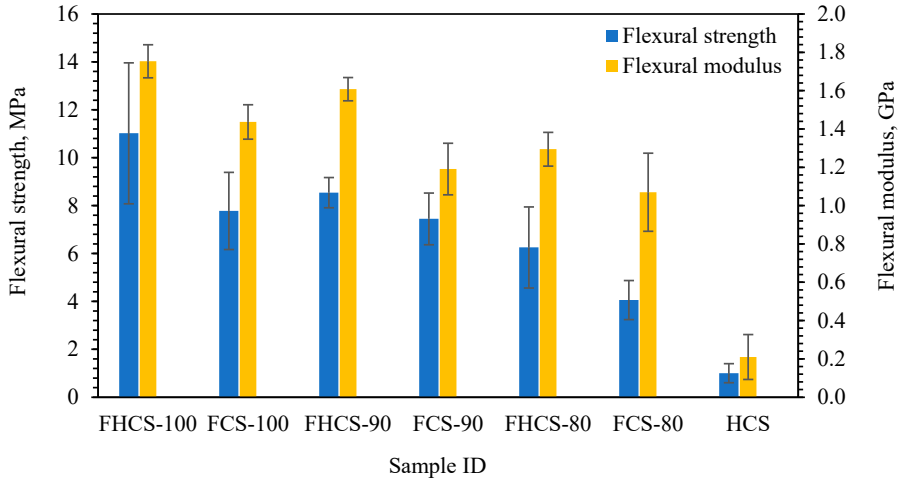


**Figure 9.** Flexural strength and modulus of various sandwich structures.

The facing stress developed in the sandwich structures during the flexural test is shown in Figure 10. Regardless of the honeycomb incorporation of the sandwich structures, the sandwiches made of high SSS concentration showed higher facing stress. The reinforcement of paper honeycomb increased the facing stress of the sandwich structures by 52.19%, 25.99%, and 51.18%, respectively, for SSS concentrations of 100%, 90%, and 80%. According to the results, the FCS-80 sandwich showed the lowest facing stress of 18.94 MPa, and the FHCS-100 sandwich showed the highest facing stress of 51.26 MPa. The facing stress increased from 4.59 MPa to a maximum of 51.26 MPa (increased by 1016.78%) due to filling the paper honeycomb core-based sandwich (HCS) with perlite/sodium silicate foam made of 100% SSS. The improvements were 765.14% and 523.75% for the perlite/sodium silicate foams made of 90% and 80% SSS, respectively. The maximum facing stress developed in the FHCS-100 sandwich was 51.26 MPa, which was 12.93% less than the tensile strength of the Formica sheet (which was 57.89 MPa, as shown in Table 1). Therefore, it can be hypothesized that any of this investigation's sandwiches, under flexural loading, must not fail by face-sheet tearing at the tension side of the specimen. The failure modes of the sandwiches are discussed later in this paper.

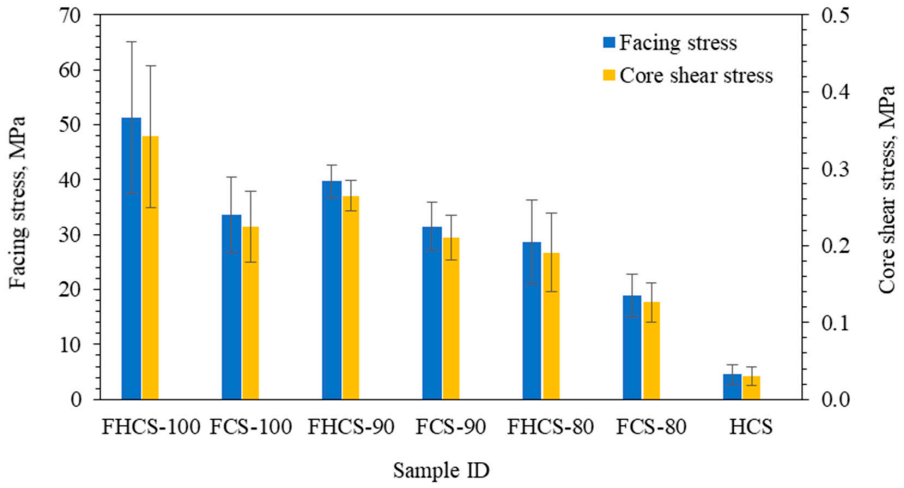


**Figure 10.** Facing stress and core shear stress of various sandwich structures.

The core shear stresses at peak load for different samples are shown in Figure 10 in the secondary axis, with standard deviations as error bars. Similar to the facing stress, the core shear stress decreased with the dilution of the SSS. The core shear stress developed in the FHCSs was also found to be higher than that of the corresponding FCSs. On

the other hand, the HCS showed a core shear stress of 0.03 MPa, and the core shear stress also increased significantly, similar to the facing stress due to filling the HCS with perlite/sodium silicate foams.

Specific properties are very important for describing lightweight materials. They are provided in Table 5. It can be seen from Table 5 that the characteristic features of specific flexural properties are similar to those of general flexural properties (as discussed above) because of the insignificant change in densities of the sandwich structures with or without a paper honeycomb. However, the specific flexural properties of both the FHCSs and the FCSs appeared to be significantly higher than that of the HCS, although the density of the HCS was considerably lower. For instance, the FHCS structure with 100% SSS concentration exhibited a 251.11% higher specific flexural strength, compared to that of the HCS structure.

**Table 5.** Specific flexural properties of the sandwich structures in this study and from the literature.

| Sample ID | Density ($g/cm^3$) | Sp. Flexural Strength, [$MPa/(g/cm^3)$)] | Sp. Flexural Modulus, [$GPa/(g/cm^3)$)] |
|---|---|---|---|
| FHCS-100 | 0.47 | 23.77 | 3.78 |
| FHCS-90 | 0.44 | 19.62 | 3.69 |
| FHCS-80 | 0.42 | 15.25 | 3.16 |
| FCS-100 | 0.46 | 17.18 | 3.17 |
| FCS-90 | 0.43 | 17.44 | 2.79 |
| FCS-80 | 0.40 | 10.15 | 2.68 |
| HCS | 0.15 | 6.77 | 1.42 |
| Portland cement skin with kraft paper honeycomb core [26] | 0.99 | 0.88 | - |
| Flax-reinforced Portland cement skin with kraft paper honeycomb core [26] | 0.89 | 1.74 | - |
| Oriented strand boards or plywood [37] | 0.55 | 29.82 | 8.97 |
| Gypsum-fiber boards [37] | 1.15 | 3.48 | 3.30 |
| Chips board urea-formaldehyde bonded [38] | 0.72 | 15.97 | 2.68 |
| MDF [38] | 0.68 | 27.50 | - |
| Coconut coir cement board [39] | 1.13 | 17.64 | 4.70 |
| Commercial flake board [39] | 1.40 | 8.43 | 4.29 |
| Commercial cellulose board [39] | 1.56 | 12.24 | 4.22 |
| Gypsum panel [11] | 1.00 | 2.26 | 2.12 |
| Jute-fiber-reinforced gypsum panel [11] | 0.97 | 2.03 | 2.24 |
| Perlite/sodium silicate foam panel [22] | 0.41 | 2.37 | 0.87 |
| Syntactic foam panel [40] | 0.37 | 21.32 | 2.86 |
| Syntactic foam panel [40] | 0.44 | 17.20 | 2.57 |
| Nylon-fiber-reinforced perlite/sodium silicate panel [18] | 0.41 | 2.68 | 0.61 |
| Perlite/sodium silicate foam with jute-fiber-reinforced epoxy composite skin [31] | 0.59 | 6.50 | 0.61 |

Table 5 also shows the specific flexural properties of some similar building materials reported in the literature. The specific flexural strength and modulus of the sandwiches developed in this work are significantly higher than those of similar building materials, including gypsum panels [11], gypsum fiber boards [37], and plywood [37]. The densities of building materials such as perlite/sodium silicate foam [22], syntactic foam [40], nylon-fiber-reinforced perlite sodium silicate foam [18], and sandwich structures made with a perlite/sodium silicate foam core with jute-fiber-reinforced epoxy composite skin [31] reported in the literature fall within the density range of the sandwiches in this work, but their specific flexural properties are comparatively lower than the sandwiches in this study. Therefore, the developed sandwich structures may be potential candidates for applications in the building industry, as non-load-bearing structures.

### *3.2. Flexural Load-Deflection Curves and Failure Mechanism*

Typical load-deflection curves and photographs of the specimens, showing the failure mode during the flexural test, are provided in Figure 11 (for FCSs) and Figure 12 (for FHCSs). All curves showed a linear increase in load, with deflections up to a peak at which the failure was initiated. The failure was not visible in the naked eye as shown in Figure 11b(i) and Figure 12b(i). The failure modes for various sandwich structures under flexural loading are summarized in Table 6. The failures were initiated by core shear cracking for all the FCSs and FHCSs, irrespective of the SSS concentrations, because of the low shear strength of the perlite/sodium silicate core. For FCSs with 100% SSS concentration, the failure sequence was found to be core shear cracking (Figure 11b(ii)) followed by a small delamination and top-skin fracture (Figure 11b(iii)). For other FCSs, the failure sequence was core shear cracking followed by the delamination of either the top or the bottom skin, or both skins, from the core. On the other hand, for all the FHCSs, the core shear cracking (Figure 12b(ii)) was followed by the top-skin fracture (Figure 12b(iii)). After careful observation of the recorded video of the flexural testing and the corresponding load–deflection curves, the portion of the curves during shear cracking, skin delamination, and skin fracture were identified. They are shown in Figure 11a for the FCSs and in Figure 12a for the FHCSs. It was observed from the load–deflection curves that the core shear and delamination caused a gradual drop in load with deflection, while the skin fracture triggered a rapid drop in the load-bearing capacity of the sandwiches. In the case of the HCS, the load increased with increasing deflection, up to a peak, followed by a gradual drop in load with increasing deflection, as shown in Figures 11a and 12b. The local deformation of the top skin initiated at the peak load, due to buckling of the paper honeycomb core, as shown in Figure 11b(iv).

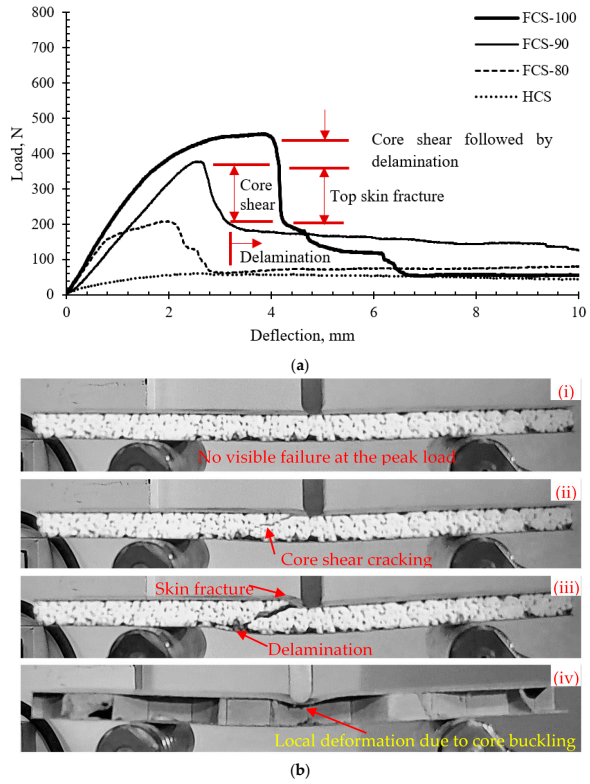


**Figure 11.** (**a**) Typical load vs. displacement curves of foam core-based sandwiches and (**b**) representative photographs of the failed sandwiches during the flexural test: (i) no visible failure at the peak load, (ii) core shear cracking, (iii) skin fracture, and (iv) local deformation due to core buckling in the paper honeycomb core-based sandwich structure.

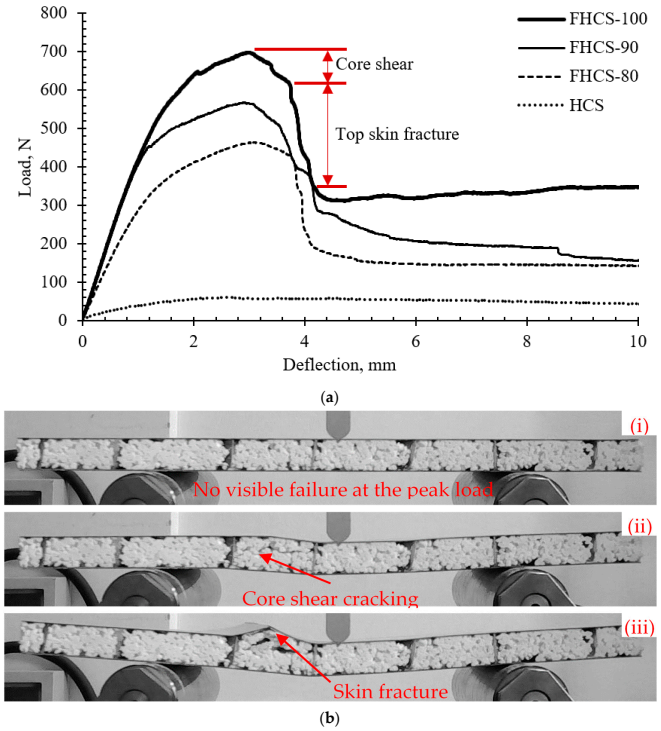


**Figure 12.** (**a**) Typical load vs. displacement curves of foam-filled honeycomb core-based sandwiches and (**b**) representative photographs showing failure modes of the sandwich during the flexural test: (i) no visible failure at the peak load, (ii) core shear cracking, and (iii) skin fracture.

**Table 6.** Summary of the failure mechanisms of various sandwich structures.

| Sample ID | Failure Sequence |
|---|---|
| FHCS-100 | Core shear–top skin fracture |
| FHCS-90 | Core shear–top skin fracture |
| FHCS-80 | Core shear–top skin fracture |
| FCS-100 | Core shear–delamination-top skin fracture |
| FCS-90 | Core shear–delamination |
| FCS-80 | Core shear–delamination |
| HCS | Local buckling of honeycomb core |

A comparison of load–deflection curves for the FHCS-100, the FCS-100, the HCS, and the combined HCS and FCS-100 are provided in Figure 13. The load-bearing ability of the FHCS was significantly higher than those of the HCS, the FCS-100, and the combined HCS and FCS-100, indicating a remarkably higher load-bearing capability of the FHCSs due to the interaction effect.

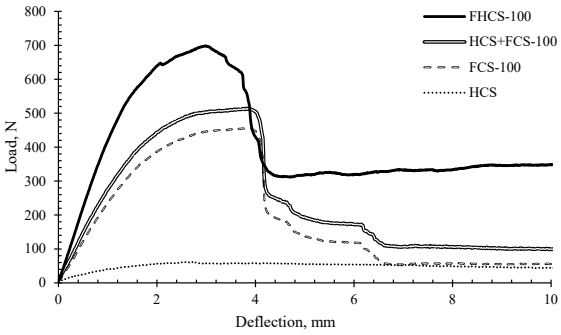


**Figure 13.** Comparison of load-deflection curves of HCS, FCS-100, combined HCS and FCS-100, and FHCS-100.

### 3.3. Thermal Behavior

The thermal conductivity of the different samples is shown in Figure 14, with the standard deviation indicated by the error bars. The range of thermal conductivity of the sandwiches, with and without paper honeycomb, was found to be from 0.095 W/mK to 0.113 W/mK. It is clear from the figure that the effects of solid content in SSS and paper honeycomb reinforcement on thermal conductivity are insignificant.

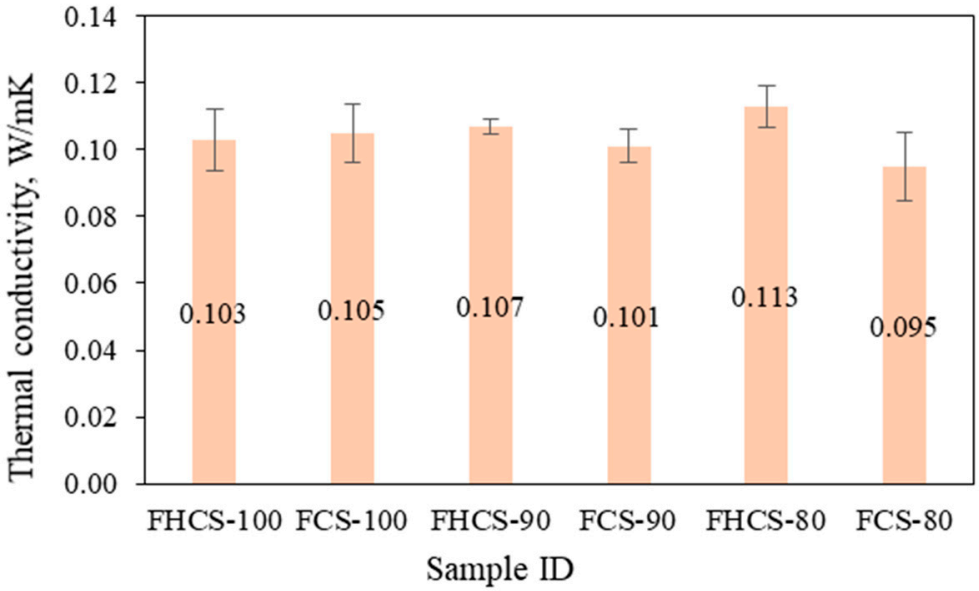


**Figure 14.** Thermal conductivity of different samples, with standard deviations as error bar.

The thermal conductivities of various non-load-bearing building materials reported in the literature, together with the results of the current study, are provided in Table 7. The thermal conductivities of MDF [38], plywood-Scots pine and black pine [41], particleboard [38], and flax-reinforced Portland cement skin with a kraft paper honeycomb core sandwich [26] fell within the range of thermal conductivity of the sandwiches reported in this work. However, the densities of those materials were significantly higher than those of the sandwiches in this work. The densities of a date palm waste-MDF sandwich panel [42], polystyrene foamed concrete [43], and cork-gypsum composite [44] were within the range of the densities of the sandwich panels in this study, but their thermal conductivities were higher than those of the sandwiches developed in this work. The gypsum board [26], gypsum fiberboard [37], oriented strand board or plywood [37], plywood (Beech) [38], coconut coir cement board [39], commercial flake and cellulose board [39], gypsum composite [45], and newspaper sandwiched ALC panel [46] possessed both higher densities and higher thermal conductivities than those of the sandwiches in the current study. Another lightweight board was manufactured by Lesiecki et al., using triticale straw for building insulation [47]. The thermal conductivity of the boards was found to be in the range from 0.033 W/mK to 0.046 W/mK, for a density range of 0.15 g/cm$^3$ to 0.20 g/cm$^3$. However, the bending properties of the boards were not provided. Therefore, the sandwiches reported in this work have a high potential for use as non-load-bearing building insulation materials because of their lower thermal conductivity and their lightweight properties.

**Table 7.** Thermal conductivity of various building materials found in the literature, together with the results of the current study.

| Reference | Materials | Density ($g/cm^3$) | Thermal Conductivity (W/m.K) |
|---|---|---|---|
| [26] | Gypsum board | 0.65 | 0.159 |
| [37] | Gypsum fiberboard | 1.15 | 0.32 |
| [38] | MDF | 0.696 | 0.0974 |
| [38] | Thin MDF | 0.802 | 0.1104 |
| [42] | Date Palm Waste-MDF sandwich panel | 0.456 | 0.1357 |
| [37] | Oriented strand boards (OSB) or plywood (PWD) | 0.65 | 0.13 |
| [38] | Plywood (Beech) | 0.679 | 0.1304 |
| [41] | Plywood (Scots pine) | 0.58 | 0.10 |
| [41] | Plywood (Black pine) | 0.60 | 0.11 |
| [38] | Particleboard | 0.597 | 0.0965 |
| [26] | Flax-reinforced Portland cement skin with kraft paper honeycomb core | 0.89 | 0.097 |
| [39] | Coconut coir cement board | 1.04 | 0.40 |
| [39] | Commercial flakeboard | 1.04 | 0.36 |
| [39] | Commercial cellulose board | 1.56 | 0.68 |
| [43] | Polystyrene foamed concrete | 0.4 | 0.157 |
| [44] | Cork–gypsum composite | 0.472 | 0.124 |
| [45] | Gypsum composite | 0.88 | 0.13 |
| [46] | Newspaper sandwiched ALC panel | 1.1 | 0.30 |
| [47] | Triticale straw board | 0.15–0.20 | 0.033–0.046 |
| Current study | Perlite/sodium silicate foam-based sandwich with Formica sheet skin | 0.40–0.47 | 0.095–0.113 |

## 4. Conclusions

Novel sandwich structures were manufactured with paper honeycomb, perlite/sodium silicate foam, and perlite/sodium silicate foam-filled paper honeycomb as the cores, with Formica sheets as the skins. The flexural behavior and the thermal conductivity of the sandwich structures were investigated. The findings of this work can be summarized as follows:

- The flexural properties of the foam-only sandwich structures improved significantly with paper honeycomb reinforcement. Paper honeycomb reinforcement can be an effective method for enhancing foam-core-based sandwich structures. Furthermore, the perlite/sodium silicate composite foam filling in the cells of the paper honeycomb core increased the flexural properties of the sandwich structures remarkably.
- The paper honeycomb core-based sandwich structure exhibited a reasonable flexural strength of 1.01 MPa, making it suitable for non-load-bearing structures.
- The density of the sandwich structures increased with the foam filling, but the specific flexural properties were substantially greater than those of the paper honeycomb core-based sandwiches.
- The failure initiation due to flexural loading in foam-only and foam-filled paper honeycomb sandwich structures occurred by core shear cracking. In contrast, the failure in the paper honeycomb core-based sandwich was found to be local deformation, due to core buckling.

- The highest facing stress developed in the sandwich structures was lower than the tensile strength of the Formica sheets. Therefore, the performance of the sandwich structures could be further improved by enhancing the shear strength of the cores.
- Core shear failure did not significantly impact the load-bearing capacity of the sandwiches. Instead, the second stages of failure, such as delamination or skin fracture, led to a rapid drop in load-bearing capacity.
- The concentration of sodium silicate and the presence of paper honeycomb reinforcement in the perlite/sodium silicate foam core-based sandwich structures had an insignificant effect on thermal conductivity.
- The thermal conductivity of the foam core-based sandwiches, with or without paper honeycomb, ranged from 0.095 to 0.113 W/mK, which was significantly lower than that of many existing building materials found in the literature.
- Additionally, the specific flexural properties of the sandwiches studied in this work were comparable to those of common building materials used in non-load-bearing applications.

**Author Contributions:** Conceptualization, M.A.; Formal analysis, F.H., M.A. and M.S.I.; Investigation, M.M.I.; Writing—original draft, F.H. and M.A.; Supervision, M.A.; Writing—review & editing, M.S.I. and M.M.I. All authors have read and agreed to the published version of the manuscript.

**Funding:** This research received no external funding.

**Data Availability Statement:** Data is contained within the article. Additional data may be made available with a reasonable request.

**Acknowledgments:** The authors acknowledge the support from the Head of the Department of Mechanical Engineering, Khulna University of Engineering & Technology, Bangladesh for allowing to work in various laboratories and the partial funding provided to the first author for undergraduate thesis from Khulna University of Engineering and Technology (KUET).

**Conflicts of Interest:** The authors declare no conflict of interest.

## References

1. Berge, B. *The Ecology of Building Materials*; Routledge: London, UK, 2009.
2. Lanzón, M.; García-Ruiz, P. Lightweight cement mortars: Advantages and inconveniences of expanded perlite and its influence on fresh and hardened state and durability. *Constr. Build. Mater.* **2008**, *22*, 1798–1806. [CrossRef]
3. Dube, W.; Sparks, L.; Slifka, A. Thermal conductivity of evacuated perlite at low temperatures as a function of load and load history. *Cryogenics* **1991**, *31*, 3–6. [CrossRef]
4. Ennis, D. Perlite mining and reclamation in the no aqua peaks, Taos County, New Mexico. In Proceedings of the 62nd Field Conference Geology of the Tusas Mountains–Ojo Caliente: New, Mexico, USA, New Mexico Geological Society Guidebook, Espanola, NM, USA, 28 September–1 October 2011.
5. Yilmazer, S.; Ozdeniz, M.B. The effect of moisture content on sound absorption of expanded perlite plates. *Build. Environ.* **2005**, *40*, 311–318. [CrossRef]
6. Rashad, A.M. A synopsis about perlite as building material—A best practice guide for Civil Engineer. *Constr. Build. Mater.* **2016**, *121*, 338–353. [CrossRef]
7. Jack, M.; Rahr, C.E. Building Board of Fiber and Asphalt Coated Perlite. U.S. Patent 2,626,864, 27 January 1953.
8. Sherman, N.; Cameron, J.H. Method of Manufacturing Improved Mineral Board. U.S. Patent 4,297,311, 27 October 1981.
9. Shastri, D.; Kim, H.S. A new consolidation process for expanded perlite particles. *Constr. Build. Mater.* **2014**, *60*, 1–7. [CrossRef]
10. Vimmrová, A.; Keppert, M.; Svoboda, L.; Černý, R. Lightweight gypsum composites: Design strategies for multi-functionality. *Cem. Concr. Compos.* **2011**, *33*, 84–89. [CrossRef]
11. Karua, P.; Arifuzzaman, M.; Islam, M.S. Effect of jute fiber reinforcement on the mechanical properties of expanded perlite particles-filled gypsum composites. *Constr. Build. Mater.* **2023**, *387*, 131625. [CrossRef]
12. Arifuzzaman, M.; Kim, H.S. Novel mechanical behaviour of perlite/sodium silicate composites. *Constr. Build. Mater.* **2015**, *93*, 230–240. [CrossRef]
13. Arifuzzaman, M.; Kim, H.S. Flatwise Compression and Flexural Behaviour of Perlite/Sodium Silicate Composite Foam. *Appl. Mech. Mater.* **2017**, *860*, 19–24. [CrossRef]
14. Arifuzzaman, M.; Kim, H.S. Prediction and evaluation of density and volume fractions for the novel perlite composite affected by internal structure formation. *Constr. Build. Mater.* **2017**, *141*, 201–215. [CrossRef]

15. Arifuzzaman, M.; Kim, H.S. Plane Stress/Strain Compressive Behavior of Perlite Composite Foam. *J. Test. Eval.* **2019**, *47*, 2905–2925. [CrossRef]
16. Adhikary, P.; Arifuzzaman, M.; Kabir, E. Compressive properties of expanded perlite based particulate composite for the application in building insulation Board. *J. Eng. Adv.* **2020**, *1*, 1–5. [CrossRef]
17. Karua, P.; Arifuzzaman, M. Compressive behavior of perlite/sodium silicate composite foam modified by boric acid. *Metall. Mater. Eng.* **2022**, *28*, 103–124. [CrossRef]
18. Aziz Naser Takey, A.S.M.; Hossain, G.M.I.; Sarker, S.; Arifuzzaman, M. Effect of Nylon Fiber Reinforcement on Mechanical Behavior of Expanded Perlite/Sodium Silicate Composites. In Proceedings of the 2nd International Conference on Mechanical Engineering and Applied Sciences (ICMEAS), MIST, Dhaka, Bangladesh, 8–12 December 2022.
19. Tian, Y.L.; Guo, X.L.; Wu, D.L.; Sun, S.B. A study of effect factors on sodium silicate based expanded perlite insulation board strength. *Appl. Mech. Mater.* **2013**, *405*, 2771–2777. [CrossRef]
20. Al Abir, A.; Faruk, M.O.; Arifuzzaman, M. Novel expanded perlite based composite using recycled expanded polystyrene for building material applications. In Proceedings of the 6th International Conference on Mechanical, Industrial and Energy Engineering (ICMIEE), KUET, Khulna, Bangladesh, 19–21 December2020.
21. Yew, M.C.; Yew, M.K.; Yuen, R.K.K. Experimental analysis of lightweight fire-rated board on fire resistance, mechanical, and acoustic properties. *Fire* **2023**, *6*, 221. [CrossRef]
22. Arifuzzaman, M.; Kim, H.S. Novel flexural behaviour of sandwich structures made of perlite foam/sodium silicate core and paper skin. *Constr. Build. Mater.* **2017**, *148*, 321–333. [CrossRef]
23. Wang, D. Impact behavior and energy absorption of paper honeycomb sandwich panels. *Int. J. Impact Eng.* **2009**, *36*, 110–114. [CrossRef]
24. Dongmei, W. Cushioning properties of multi-layer corrugated sandwich structures. *J. Sandw. Struct. Mater.* **2009**, *11*, 57–66. [CrossRef]
25. Chen, Z.; Yan, N. Investigation of elastic moduli of Kraft paper honeycomb core sandwich panels. *Compos. Part B Eng.* **2012**, *43*, 2107–2114. [CrossRef]
26. Shahbazi, S.; Singer, N.; Majeed, M.; Kavgic, M.; Foruzanmehr, R. Cementitious Insulated Drywall Panels Reinforced with Kraft-Paper Honeycomb Structures. *Buildings* **2022**, *12*, 1261. [CrossRef]
27. Fu, Y.; Sadeghian, P. Flexural and shear characteristics of bio-based sandwich beams made of hollow and foam-filled paper honeycomb cores and flax fiber composite skins. *Thin-Walled Struct.* **2020**, *153*, 106834. [CrossRef]
28. Abd Kadir, N.; Aminanda, Y.; Ibrahim, M.S.; Mokhtar, H. Experimental study on energy absorption of foam filled kraft paper honeycomb subjected to quasi-static uniform compression loading. *IOP Conf. Ser. Mater. Sci. Eng.* **2016**, *152*, 012048. [CrossRef]
29. Abd Kadir, N.; Aminanda, Y.; Ibrahim, M.S.; Mokhtar, H. Experimental study of low-velocity impact on foam-filled Kraft paper honeycomb structure. *IOP Conf. Ser. Mater. Sci. Eng.* **2018**, *290*, 012082. [CrossRef]
30. Safarabadi, M.; Haghighi-Yazdi, M.; Sorkhi, M.; Yousefi, A. Experimental and numerical study of buckling behavior of foam-filled honeycomb core sandwich panels considering viscoelastic effects. *J. Sandw. Struct. Mater.* **2021**, *23*, 3985–4015. [CrossRef]
31. Sarkar, S.; Aziz Naser Takey, A.S.M.; Ahammad, R.; Islam, M.S.; Arifuzzaman, M. Mechanical behavior of sandwich structure made of perlite foam core and JFRP skin. In Proceedings of the 7th International Conference on Mechanical, Industrial and Energy Engineering (ICMIEE), KUET, Khulna, Bangladesh, 22–24 December 2022.
32. Hossain, G.M.I.; Karua, P.; Arifuzzaman, M. Mechanical Characterization of Novel Sandwich Structures Made of Perlite/Epoxy Core with JFRP Facings. In Proceedings of the 7th International Conference on Engineering Research, Innovation and Education (ICERIE), SUST, Sylhet, Bangladesh, 12–14 January 2023.
33. Zenkert, D. *An Introduction to Sandwich Structures, Student Edition*; DTU Mechanical Engineering, Technical University of Denmark: Lyngby, Denmark, 2005.
34. Pflug, J.; Vangrimde, B.; Verpoest, I.; Bratfisch, P.; Vandepitte, D. Continuously produced honeycomb cores. In Proceedings of the International SAMPE Symposium and Exhibition, Long Beach, CA, USA, 11–15 May 2003.
35. *ASTM C393/C393M-11*; Standard Test Method for Core Shear Properties of Sandwich Constructions by Beam Flexure. ASTM International: West Conshohocken, PA, USA, 2016.
36. Barragán, V.M.; Maroto, J.C.; Pastuschuk, E.; Muñoz, S. Testing a simple Lee's disc method for estimating throuh-plane thermal conductivity of polymeric ion-exchange membranes. *Int. J. Heat Mass Transf.* **2022**, *184*, 122295. [CrossRef]
37. Casagrande, D.; Grossi, P.; Tomasi, R. Shake table tests on a full-scale timber-frame building with gypsum fibre boards. *Eur. J. Wood Wood Prod.* **2016**, *74*, 425–442. [CrossRef]
38. Thoemen, H.; Irle, M.; Sernek, M. (Eds.) *Wood-Based Panels: An Introduction for Specialists*; Brunel University Press: London, UK, 2010.
39. Asasutjarit, C.; Hirunlabh, J.; Khedari, J.; Charoenvai, S.; Zeghmati, B.; Cheul Shin, U. Development of coconut coir-based lightweight cement board. *Constr. Build. Mater.* **2007**, *21*, 277–288. [CrossRef]
40. Islam, M.M.; Kim, H.S. Sandwich composites made of syntactic foam core and paper skin: Manufacturing and mechanical behavior. *J. Sandw. Struct. Mater.* **2012**, *14*, 111–127. [CrossRef]
41. Demirkir, C.; Colakoglu, G.; Colak, S.; Aydin, I.; Candan, Z. Influence of aging procedure on bonding strength and thermal conductivity of plywood panels. *Acta Phys. Pol. A* **2016**, *129*, 1230–1234. [CrossRef]

42. Haseli, M.; Layeghi, M.; Hosseinabadi, H.Z. Characterization of blockboard and battenboard sandwich panels from date palm waste trunks. *Measurement* **2018**, *124*, 329–337. [CrossRef]
43. Sayadi, A.A.; Tapia, J.V.; Neitzert, T.R.; Charles Clifton, G. Effects of expanded polystyrene (EPS) particles on fire resistance, thermal conductivity and compressive strength of foamed concrete. *Constr. Build. Mater.* **2016**, *112*, 716–724. [CrossRef]
44. Cherki, A.-b.; Remy, B.; Khabbazi, A.; Jannot, Y.; Baillis, D. Experimental thermal properties characterization of insulating cork–gypsum composite. *Constr. Build. Mater.* **2014**, *54*, 202–209. [CrossRef]
45. San-Antonio-González, A.; Del Río Merino, M.; Arrebola, C.V.; Villoria-Sáez, P. Lightweight material made with gypsum and extruded polystyrene waste with enhanced thermal behaviour. *Constr. Build. Mater.* **2015**, *93*, 57–63. [CrossRef]
46. Ng, S.-C.; Low, K.-S. Thermal conductivity of newspaper sandwiched aerated lightweight concrete panel. *Energy Build.* **2010**, *42*, 2452–2456. [CrossRef]
47. Lesiecki, M.; Kawalerczyk, J.; Derkowski, A.; Wieruszewski, M.; Dziurka, D.; Mirski, R. Properties of lightweight insulating board produced from triticale straw particles. *Materials* **2023**, *16*, 5272. [CrossRef]